Electron Interference Effects in Quantum Wells: Observation of Bound and Resonant States

M. Heiblum, M. V. Fischetti, W. P. Dumke, D. J. Frank, I. M. Anderson, C. M. Knoedler, and L. Osterling

IBM Thomas J. Watson Research Center, Yorktown Heights, New York 10598

(Received 6 November 1986)

Quasimonoenergetic ballistic electrons were injected into GaAs potential wells of various thicknesses (29–72 nm). Strong modulation in the injected currents, as a function of the injection energy, was observed and correlated with electron coherence effects. A self-consistent solution of Poisson and Schrödinger equations was needed to relate these effects to the bound and, in particular, resonant quantum states in the well. The good match with theory justified the use (and led to an expression) of the electron "energy effective mass" in the central valley, in an energy range where nonparabolicity and valley transfer are significant and make this determination, usually, difficult.

PACS numbers: 71.25.Jd, 71.50.+t, 73.40.Gk

The construction of quasimonoenergetic hot electron injectors with a variable injection energy[1,2] recently made possible the direct observation of ballistic electron transport in heavily doped GaAs.[3,4] The fraction of the injected electrons traversing the layers ballistically decreased from 75% to 15% as layer thickness increased from 29 to 72 nm.[4] The thinness of the GaAs layers makes the energy spacings among the energy subbands comparable to the ballistic-electron distribution width, and since phase coherence is maintained by the ballistic electrons, quantum size effects become important. We have measured strong modulation in the currents injected into thin confined GaAs layers as a function of the injection energy. An exact, self-consistent solution of the Poisson and Schrödinger equations for the potential in the GaAs wells confirmed that the observed peaks at injection energies lower than the confining potential were associated with the bound states, while those at higher energies resulted from the resonant (virtual[5]) states in the continuum energy range. These coherent effects were consistent with the GaAs Γ-band nonparabolicity in the 0–0.4-eV energy range. Previously, bound states in very thin quantum wells, < 10 nm, were observed via transport measurements,[6,7] but the resonant states were not. These states had previously been studied only in multiple quantum wells via optical techniques such as excitation spectroscopy,[8] resonant Raman scattering,[9] and photoluminescence measurements.[10]

The generation of the ballistic electron beams as well as transport through thin wells were done with GaAs-$Al_xGa_{1-x}As$ (or AlGaAs) heterostructure tunneling hot electron transfer amplifier (THETA) devices.[1,2] The structures were grown by molecular-beam epitaxy and are described schematically in Fig. 1: n^+ GaAs (emitter), undoped thin AlGaAs ($\simeq 10$ nm tunnel barrier), n^+ GaAs (29–72 nm base well), undoped graded AlGaAs ($\simeq 100$ nm collector barrier), and n^+ GaAs (collector). The emitter tunnel injector produces a forward-moving narrow electron beam ($\simeq 60$ meV wide) in the well with a mean energy determined by the applied biasing voltage between base and emitter, V_{BE}. The thick AlGaAs barrier (with a potential height Φ_C) prevents tunneling of electrons with energy lower than Φ_C out of the well. For an injection energy lower than the confining potential, $eV_{BE}+\zeta < \Phi_C$, where ζ is the Fermi energy in the base on the collector side and e is the electron charge, the tunneling electrons *sense* the bound states in the base quantum well. Similarly, for $eV_{BE}+\zeta > \Phi_C$, the extended resonant states (resulting from the small but finite reflection of the ballistic hot electrons at potential discontinuities) are expected to affect the tunneling current into base and collector.

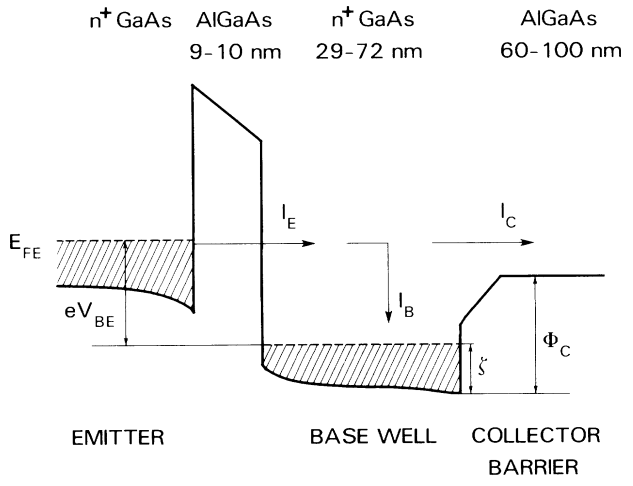

FIG. 1. A schematic diagram of the potential energy in the heterostructure device, showing the thin AlGaAs tunnel-barrier injector and the thin, heavily doped GaAs quantum well with a confining potential Φ_C. I_E and I_C are the injected (from the emitter) and collected currents, respectively. The base (well) current $I_B = I_E - I_C$ originates from the quasiballistic or reflected electrons.

In Fig. 2 experimental and theoretical results are shown for three structures with different well widths (72, 51.5, and 29 nm, all doped to a level of 1×10^{18} cm^{-3}) and different confining potentials, Φ_C (0.23, 0.33, and 0.14 eV), determined by the Al mole fraction, x, in the collector barrier. Measurements were done at 4.2 K, for a grounded base and collector-to-base voltage $V_{CB}=0$. The heavy solid lines representing the derivative of the measured injected currents I_E exhibit modulation effects as a function of the injection energy, eV_{BE}. In the first two structures only the bound energy range is monitored, while in the third structure the unbound range is monitored, too. The thin broken lines are the calculated emitter-to-base tunneling probability, T_{eb}, for an electron at the Fermi energy of the emitter. They have been obtained by our computing numerically the charge density of the electrons that tunneled into the well and dividing it by the charge density associated with the incident wave in the emitter. The potential energy $eV(x)$ and the free-electron distribution $n(x)$, shown in Fig. 3(a), were obtained by integration of the Poisson equation with the classical charge density, as shown for a 30-nm well device that will be discussed later in Fig. 4(b). Nonparabolicity effects have been included by use of the "energy effective mass," $m(E)=\hbar^2k^2/2E(k)$, where $\hbar$ is the reduced Planck's constant, k is the electron wave vector, and $E(k)$ is the electron dispersion relation in the (100) direction obtained from empirical-pseudopotential band-structure calculations.[11] In these calculations a Γ-to-L band splitting of 0.32 eV and an effective mass $m(E=0)=0.067m_0$ (m_0 being the free-electron mass) were enforced. This mass, and not the so-called "optical effective mass," $m_{\rm opt}(E)=\hbar^2k[dE(k)/dk]^{-1}$, is appropriate for the calculation of energy levels in quantum wells.[12] For the effective mass of the electrons in the AlGaAs we have used $m=m_0(0.067+0.0835x)$.[13]

The agreement between the position of the calculated transmission and measured peaks in the 72-nm and 51.5-nm well structures is excellent, indicating that we did indeed observe the bound states in the wells. It confirms the validity of the nonparabolicity used at energies as high as 0.2 eV in the Γ band. For the 29-nm well structure, however, the agreement between experimental results and the "classical" solution is poor. Here, the confinement of the electrons in the well results in a substantial modification of the charge distribution, the position of the Fermi level ζ, and the resultant potential well.

Figure 3(b) illustrates the effect of well quantization on $eV(x)$ and $n(x)$ in the 30-nm well device. The potential energy shown has been obtained by integration of the Poisson and Schrödinger equations self-consistently with a standard iterative procedure,[14] with the assumption that the electronic wave functions vanish at the outer ends of the confining barriers. This assumption is not rigorously correct, particularly for the high-lying states, but its effect on the charge and potential distributions associated with the deepest (occupied) levels is negligibly small. The major features to be noticed in the self-consistent solution are the peaked charge density in the center of the well region and the higher Fermi level ζ (ζ

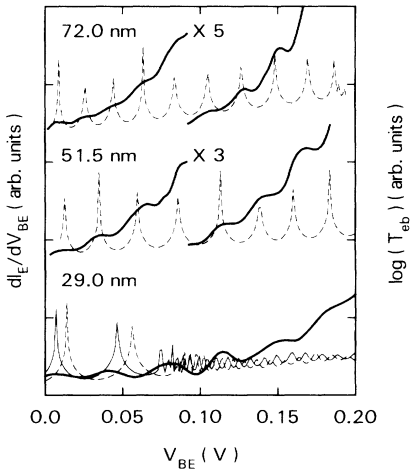

FIG. 2. The measured derivative of the injected currents at 4.2 K and $V_{CB}=0$ (solid heavy lines; note the $\times5$ and $\times3$ factors in the low voltage range), and the calculated logarithm of the transmission, T_{eb}, into 72-, 51.5-, and 29-nm-wide wells. The broken lines are the results for a classical potential while the solid thin line (for the 29-nm well device) is for the self-consistent potential.

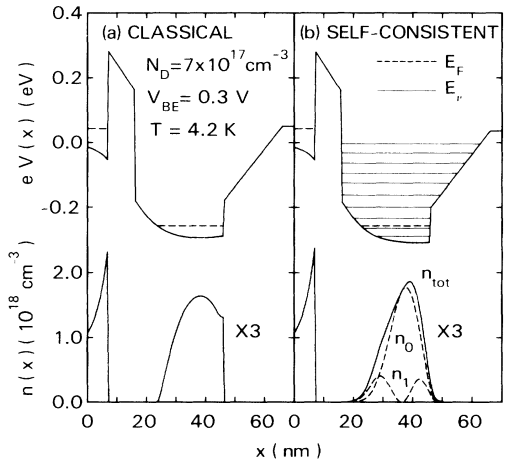

FIG. 3. The potential energy distribution, $eV(x)$, and carrier concentration, $n(x)$, through a device with a 30-nm well width, doping of 7×10^{17} cm^{-3}, $V_{CB}=0$, and $\Phi_C=0.34$ eV. Undoped GaAs spacers, 2 nm wide, were introduced on each side of the AlGaAs barriers. Calculation done (a) with the classical charge distribution and (b) by self-consistent solution of the Poisson and Schrödinger equations. The position of the Fermi level, E_F, indicates that two subbands in the well—with energy E_v ($v=0,1$)—are occupied.

is 51 meV, while only 33 meV in the classical solution). The calculated transmission in the self-consistent potential in the 29-nm well structure is shown by the thin solid line at the bottom of Fig. 2. The positions of the large, widely spaced peaks representing the tunneling into the bound states match fairly well the maxima in the derivative of the injected current. The small, closely spaced peaks (for $V_{BE} \geq 80$ meV) represent unbound states in the collector barrier due to interference effects in it. Because of these peaks, the wider spaced modulation associated with the virtual states in the well is difficult to identify. In the experiments these closely spaced oscillations are not observed because of small fluctuations in the barrier thickness and the finite width of the ballistic distribution.

The quasimonoenergetic nature of the ballistic electrons is included in the calculation of the current density $J_\gamma(V_\gamma)$ (γ is emitter-collector or emitter-base) by our integrating numerically the tunneling probabilities, T_γ, over the electron flux in the emitter at the tunnel-barrier interface. Accounting for the unoccupied states in the well and for tunneling in the reverse direction we get

$$J_\gamma(V_\gamma) \propto \int_0^\infty dR \frac{\rho(E)}{[2Em(E)]^{1/2}} [f(E) - f(E+eV_\gamma)] \int_0^E dE_\perp T_\gamma(E_\perp, V_\gamma). \quad (1)$$

Here $\rho(E)$ is the density of states in the emitter, $f(E)$ is the Fermi function in the emitter, and $E_\perp = \hbar^2 k_\perp^2 / 2m(E)$ is the "normal" electron energy, $k_\perp$ being the component of the electron wave vector normal to the tunnel-barrier interface. Finally, the numerical derivatives of the logarithm of Eq. (1) with respect to the bias V_{BE} have been taken to make a comparison with the experimental data, as shown in Fig. 4(a). A good agreement is found between the positions of the experimentally measured and the calculated peaks. The absolute magnitude of the peaks is more difficult to estimate because of other sources of current flow, aside from the elastic tunneling component, such as through defects in the thin AlGaAs barrier and via etched surfaces. The measured peaks are wider than theoretically expected, most probably because of unavoidable fluctuations (of about a couple of monolayers) in tunnel barrier and well thicknesses.

A wider energy range is probed in the structure described in Fig. 3. It has a 30-nm well, doping density of 7×10^{17} cm^{-3}, and a confining potential of $\Phi_C = 0.34$ eV. With use of the self-consistent potential [shown in Fig. 3(b)], an excellent agreement with the measured peak positions of dI_E/dV_{BE} is seen over the entire energy range in Fig. 4(b). This confirms electron coherence and nonparabolicity effects up to an energy of 0.4 eV in the Γ band. Note also that in all structures similar modulation effects were observed in the collector current, I_C, for a fixed $V_{CB} = 0$, in the unbound energy range.

Since the position of the calculated peaks is most sensitive to the energy effective mass $m(E)$, the results for it as obtained directly from our calculated band structure are accurate to a few percent, and can be expressed in the energy range 0 to 0.4 eV by

$$m(E) = 0.067 m_0 (1 - aE); \quad a = -0.834 \text{ eV}^{-1}. \quad (2)$$

Our value for the nonparabolicity coefficient is different from commonly used values, $a = -0.610$ eV^{-1} (Littlejohn, Hauser, and Glisson[15]) or $a = -0.542$ eV^{-1} (Blakemore[16]). The calculated energy effective mass is that of the Γ-band ballistic electrons, since only they maintain coherence and participate in the interference effects.[17] In general, however, at this energy range, measured effective mass is an average of masses in the Γ and L valleys.

A much simplified, if less exact, theoretical approach is to use a WKB-like integration of the phase of a ballistic electron in the well. The condition for a state (or a standing electron wave) is given by $\int_{well} k_\perp(x) dx = 2\pi N$, where N is an integer. If, for the bound states, the point of reflection is taken at the end of the base and for the unbound states at the peak of the collector barrier, the spacings are predicted with roughly a 10% error.

These quantization effects can be important not only for the kinematics we discuss in the present paper, but

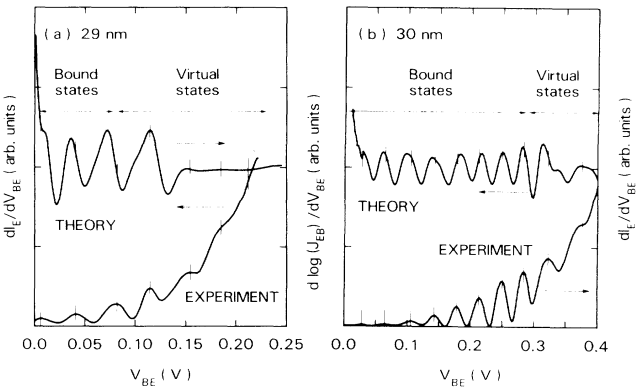

FIG. 4. The derivative of the measured injected currents, at 4.2 K and $V_{CB} = 0$, into two similar wells with different confining potentials, (a) $\Phi_C = 140$ meV and (b) $\Phi_C = 340$ meV. The calculated derivative of the currents was obtained in the self-consistent potential by use of Eq. (1) in the text. The virtual states are defined when the energy of the conduction band in the emitter crosses the energy $e\Phi_C$. Note that the theoretical broadening is due to the smoothing needed to obtain the numerical derivative of $\log J_{BE}$.

also for the dynamics of the injected electrons. These electrons, while traversing the thin base region, lose energy predominantly to the coupled phonons and two-dimensional plasmon modes,[18] which are likely to engender a dispersion significantly different from the bulk modes. Consequently, the scattering affecting the transport of ballistic electrons through thin regions is expected to be quite different from that in the bulk.

In summary, coherent interference effects of ballistic electrons were observed via transport in heavily doped GaAs quantum wells, 29–72 nm wide. Bound and unbound or virtual states in wells were observed. Their calculated values, based on a self-consistent, quantized solution for the potential in the wells together with nonparabolicity derived directly from pseudopotential band-structure calculations, were in excellent agreement with the observed data over an energy range 0–0.4 eV. We have found that the energy effective mass, with a nonparabolicity coefficient $a = -0.834\ \mathrm{eV}^{-1}$, is the appropriate mass to use, and not the optical effective mass that is commonly used in quantum-well calculations.

We thank R. Collins, A. B. Fowler, T. W. Hickmott, E. E. Mendez, F. Stern, and G. C. Wilson for their comments on the manuscript.

[1]M. Heiblum, Solid State Electron. **24**, 343 (1981).

[2]N. Yokoyama, K. Imamura, T. Ohshima, H. Nishi, S. Muto, K. Kondo, and S. Hiyamizu, in *Technical Digest of the International Electron Device Meeting, San Francisco, California, 1984* (IEEE, New York, 1984), p. 532.

[3]M. Heiblum, M. I. Nathan, D. C. Thomas, and C. M. Knoedler, Phys. Rev. Lett. **55**, 2200 (1985).

[4]M. Heiblum, I. M. Anderson, and C. M. Knoedler, Appl. Phys. Lett. **49**, 207 (1986).

[5]D. Bohm, *Quantum Theory* (Prentice-Hall, New York, 1951), Pt. 3.

[6]H. Morkoç, J. Chen, U. K. Reddy, and S. Luryi, Appl. Phys. Lett. **49**, 70 (1986).

[7]E. E. Mendez, E. Calleja, C. E. T. Gonçalves da Silva, L. L. chang, and W. I. Wang, Phys. Rev. B **33**, 7368 (1986).

[8]G. Bastard, U. O. Ziemelis, C. Delalande, M. Voos, A. C. Gossard, and W. Weigmann, Solid State Commun. **49**, 671 (1984).

[9]J. E. Zucker, A. Pinczuk, D. S. Chemla, A. Gossard, and W. Weigmann, Phys. Rev. B **29**, 7065 (1984).

[10]J. J. Song, Y. S. Yoon, P. S. Jung, A. Fedotowsky, J. N. Schulman, C. W. Tu, R. F. Kopf, D. Huang, and H. Morkoç, in Proceedings of the International Conference on Physics of Semiconductors, Stockholm, Sweden, 1986 (to be published).

[11]Marvin L. Cohen and T. K. Bergstresser, Phys. Rev. **141**, 789 (1966).

[12]T. Hiroshima and R. Lang, Appl. Phys. Lett. **49**, 456 (1986).

[13]S. Adachi, J. Appl. Phys. **58**, R1 (1985).

[14]F. Stern, J. Comput. Phys. **6**, 56 (1970). Note that the potential in the accumulation layer in the emitter was calculated classically; this is a reasonable approximation because of the small band bending.

[15]M. A. Littlejohn, J. R. Hauser, and T. H. Glisson, J. Appl. Phys. **48**, 4587 (1977).

[16]J. S. Blakemore, J. Appl. Phys. **53**, R123 (1982).

[17]M. Heiblum, E. Calleja, W. P. Dumke, I. M. Anderson, and C. M. Anderson, Phys. Rev. Lett. **56**, 2854 (1986).

[18]See, for instance, David A. Dahl and L. J. Sham, Phys. Rev. B **16**, 651 (1977); M. A. Hollis, S. C. Palmateer, L. F. Eastman, L. V. Dandekar, and P. M. Smith, IEEE Electron Device Lett. **4**, 440 (1983); A. F. Levi, J. R. Hayes, P. M. Platzman, and W. Wiegmann, Phys. Rev. Lett. **55**, 2071 (1985).